

# Spatially restricted expression of *PIOtp*, a *Paracentrotus lividus Orthopedia*-related homeobox gene, is correlated with oral ectodermal patterning and skeletal morphogenesis in late-cleavage sea urchin embryos

Maria Di Bernardo<sup>2</sup>, Stefania Castagnetti<sup>1,\*</sup>, Daniela Bellomonte<sup>1</sup>, Paola Oliveri<sup>1,‡</sup>, Raffaella Melfi<sup>1</sup>, Franco Palla<sup>2</sup> and Giovanni Spinelli<sup>1,§</sup>

<sup>1</sup>Dipartimento di Biologia Cellulare e dello Sviluppo (Alberto Monroy), Università di Palermo, Viale delle Scienze, 90128 Palermo, Italy

<sup>2</sup>Istituto di Biologia dello Sviluppo del CNR, Via Ugo La Malfa 153, 90146 Palermo, Italy

\*Present address: European Molecular Biology Laboratory, Meyerhofstrasse 1, 69117 Heidelberg, Germany

‡Present address: Caltech, Division of Biology 156-29, Pasadena, 91126 CA, USA

§Corresponding author (e-mail: spinelli@mbox.unipa.it)

Accepted 24 February; published on WWW 19 April 1999

## SUMMARY

Several homeobox genes are expressed in the sea urchin embryo but their roles in development have yet to be elucidated. Of particular interest are homologues of homeobox genes that in mouse and *Drosophila* are involved in patterning the developing central nervous system (CNS). Here, we report the cloning of an *orthopedia* (*Otp*)-related gene from *Paracentrotus lividus*, *PIOtp*. *Otp* is a single copy zygotic gene that presents a unique and highly restricted expression pattern. Transcripts were first detected at the mid-gastrula stage in two pairs of oral ectoderm cells located in a ventrolateral position, overlying primary mesenchyme cell (PMC) clusters. Increases in both transcript abundance and the number of *Otp*-expressing cells were observed at prism and pluteus stages. *Otp* transcripts are symmetrically distributed in a few ectodermal cells of the oral field. Labelled cells were observed close to sites of active skeletal rod growth (tips of the budding oral and anal arms), and at the juxtaposition

of stomodeum and foregut. Chemicals known to perturb PMC patterning along animal-vegetal and oral-aboral axes altered the pattern of *Otp* expression. Vegetalization by LiCl caused a shift in *Otp*-expressing cells toward the animal pole, adjacent to shifted PMC aggregates. Nickel treatment induced expression of the *Otp* gene in an increased number of ectodermal cells, which adopted a radialized pattern. Finally, ectopic expression of *Otp* mRNA affected patterning along the oral-aboral axis and caused skeletal abnormalities that resembled those exhibited by nickel-treated embryos. From these results, we conclude that the *Otp* homeodomain gene is involved in short-range cell signalling within the oral ectoderm for patterning the endoskeleton of the larva through epithelial-mesenchymal interactions.

Key words: *Orthopedia*, Ectopic expression, Cell specification, Spiculogenesis, *Paracentrotus lividus*

## INTRODUCTION

In the sea urchin embryo the animal-vegetal (A-V) axis is established during oogenesis, and normal development relies on the presence of both maternal determinants and an extensive series of programmed cell-cell interactions. Studies on cell lineage and blastomere recombination experiments have demonstrated that micromeres, located at the most vegetal pole, develop autonomous programs of gene expression and act as a powerful signalling centre, able to specify all the blastomeres that are in contact with them (Hörstadius, 1973; Ransick and Davidson, 1993). Maternal determinants are also thought to be active in the animal region, as some ectoderm-specific genes are expressed autonomously (Reynolds et al., 1992; Ghigliione et al., 1993). However, ectoderm restricted expression of the zygotic homeobox-containing gene, *Hbox12*,

requires interaction with adjacent blastomeres and is suppressed in dissociated cells (Di Bernardo et al., 1995).

Much less is known about oral-aboral (O-A) axis specification. Although aboral specific genes are expressed at early blastula stages (Cox et al., 1986; Tomlinson and Klein, 1990), the ultimate fate of oral and aboral ectodermal cells and that of the ciliated band at their border is not fixed until the beginning of gastrulation. This time corresponds to the end of  $\text{NiCl}_2$  sensitivity.  $\text{NiCl}_2$  is a ventralizing agent that changes the fate of ectodermal cells along the O-A axis (Hardin et al., 1992). At the mid-gastrula stage, the embryo's polarity along this axis is indicated by a group of primary mesenchyme cells (PMCs) that cluster in the ventrolateral blastocoele, forming the first nucleus of spiculogenesis. Several lines of evidence have demonstrated that correct skeletal patterning is strictly dependent on interactions between PMCs and the surrounding

ectodermal wall (Ettensohn and McClay, 1986; Armstrong et al., 1993; Ettensohn and Malinda, 1993; Guss and Ettensohn, 1997). Consequently, regulatory genes specifically expressed in some ectodermal compartments should play an essential role in interpreting O-A axis information and in patterning the skeleton.

Molecular genetic evidence from a broad range of developmental systems points to the role of homeodomain transcription factors in the control of cell fate and in the subdivision of the embryo into distinct spatial domains (McGinnis and Krumlauf, 1992; Manak and Scott, 1994). Homeobox genes of both the Hox complex and the dispersed superclasses are expressed in the non-segmented sea urchin embryo (Dolecki et al., 1988; Di Bernardo et al., 1994). Spatially restricted expression of homeobox genes occurs in early (Gan et al., 1995; Di Bernardo et al., 1995) and late cleavage embryos (Angerer et al., 1989; Martinez and Davidson, 1997; Dobias et al., 1997; Bellomonte et al., 1998), suggesting that they might be involved in early events of cell lineage specification and in the differentiation of distinct cell types. Due to a relative lack of genetic tools in sea urchin, investigation of gene function relies on microinjection of wild-type or mutant synthetic mRNAs into developing embryos (Cameron et al., 1994; Ramachandran et al., 1997). Utilizing this approach, members of the wnt pathway have been implicated in A-V axial patterning and in establishing correct ectoderm-endoderm boundaries (Emily-Fenouil et al., 1998). In addition, similar studies suggest that the homeobox gene *Otx*, related to *orthodenticle*, is involved in the differentiation of aboral ectoderm cells (Mao et al., 1996; Gan et al., 1995). A member of the *Msx* homeodomain family has been implicated in specification of the vegetal plate, and patterning of primary and secondary mesenchyme cells (Dobias et al., 1997; Tan et al., 1998).

Of particular interest are sea urchin homeobox genes homologous to genes in mouse and *Drosophila* that show spatially restricted expression in the developing brain, as sea urchin larvae have no heads. Two such genes have been cloned from *S. purpuratus* embryos. They are *Otx* (Gan et al., 1995) and *Otp*, an *orthopedia* homologue (Simeone et al., 1994). Nothing is known concerning expression or function of sea urchin *Otp*. In *Drosophila* and mouse embryos, *Otp* is expressed in restricted domains of the developing central nervous system (CNS), and in *Drosophila* it is also expressed during gastrulation (Simeone et al., 1994). To investigate the role of *Otp* in sea urchins, we have cloned an *Otp* homologue from a *Paracentrotus lividus* cDNA library (*PIOtp*) and examined its expression in both normal and perturbed embryos. In addition, we have analyzed the phenotype of embryos microinjected with *Otp* mRNA. Our results strongly suggest a role for *PIOtp* in transmitting pattern information within the oral ectoderm.

## MATERIALS AND METHODS

### Embryo culture

Adults of *Paracentrotus lividus* and *Spherechinus granularis* were collected along the Sicilian coast and either maintained in a tank at 15°C or utilized immediately. Fertilization was carried out as described (Giudice, 1973) and embryos were cultured at 18°C till the desired stage. For vegetalization, embryos were raised in 30 mM LiCl

until mesenchyme blastula stage, then cultured in MFSW (Millipore Filtered Sea Water) (Ghiglione et al., 1993). To perturb the oral-aboral axis, 0.5 mM NiCl<sub>2</sub> was added to the embryo culture soon after fertilization (Hardin et al., 1992).

### Library screening and cDNA isolation

2×10<sup>5</sup> plaques of an amplified *P. lividus* prism cDNA library in a Zap express lambda vector (Stratagene) were screened with *S. purpuratus* <sup>32</sup>P-labelled *Otp* cDNA (Simeone et al., 1994). Hybridization was carried out overnight at 65°C in 6× SSC, 5× Denhardt's solution, 0.2% SDS (1× SSC is 0.15 M NaCl, 0.015 M sodium citrate, pH 7.0). Filters were washed at the same temperature in SSC of decreasing concentrations up to 0.5× SSC and exposed to X-ray films. Positive plaques were isolated, and the Bluescript recombinant plasmids prepared according to the manufacturer's protocol. Sequencing of both strands of the cDNA was carried out with the Sequenase sequencing kit (USB) and specific primers.

### DNA and RNA purification and blot hybridization

Genomic DNA, extracted from sperm of three different adults, was digested with *Eco*RI restriction enzyme, blotted onto nylon filters (Hybond N, Amersham) and hybridized at 65°C in 6× SSC with a 0.6 kb *Xho*I-*Xho*I <sup>32</sup>P-labelled *P. lividus* *Otp* cDNA fragment. Total RNA was extracted from embryos at different developmental stages and from adult tissues according to Chomczynski and Sacchi (1987). RNA blot hybridization was carried out as described (Di Bernardo et al., 1995) with a 0.6-kb in vitro-transcribed <sup>32</sup>P-labelled antisense RNA.

### Whole-mount in situ hybridization

Embryos at selected stages were fixed in 2.5% glutaraldehyde, 0.14 M NaCl, 0.2 M phosphate buffer, washed, dehydrated up to 70% ethanol and kept at -20°C. Digoxigenin 11-UTP sense and antisense RNAs were transcribed in vitro from a linearized Bluescript plasmid containing an *Otp* cDNA insert of 600 bp using the appropriate RNA polymerase. All pre-hybridization and hybridization steps were carried out as previously described (Di Bernardo et al., 1995), with slight modifications. Fixed embryos were rehydrated, digested with 30 µg/ml Proteinase K for 15 minutes at 37°C, and hybridized in sealed capillaries with 30 ng/ml of RNA probe for 16 hours at 55°C. After hybridization, embryos were washed, in several steps, in 1× SSC, 0.1% Tween-20 and 0.1× SSC, 0.1% Tween-20 at 65°C. Following antibody reaction and staining, embryos were mounted on glass slides, examined with a Zeiss Axioscope microscope and photographed using either a Kodak gold colour film 100 ASA or colour reversal film Ektachrome EPY 64 T. Photo and slide images were processed with a scanner using Adobe Photoshop software.

### Plasmid constructions for microinjection and in vitro transcription

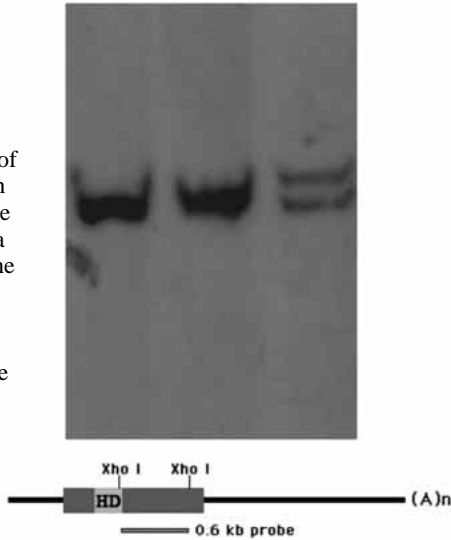
The CS2+MT expression vector (Turner and Weintraub, 1994) was used to clone amplified fragments from the *PIOtp* cDNA. This plasmid contains six copies of 39 nt encoding for a myc epitope tag, downstream of which the cDNA coding sequence, or parts of it, were cloned after PCR amplification. Oligonucleotide primers were as follows. TAGGATGGAACGAACATTAG (O1, nucleotides 319-338) and ATCATCTAAAGATACCGTTG (O2, nucleotides 1399-1418) were used to amplify the entire ORF; O1 and TGAATCG-AGTGCATGTCG, spanning nucleotides 673-692, amplified the 373-bp 5' cDNA fragment; GAAGACCACTAATGTATTTCG (nt 846-866) and O2 amplified the 571-bp 3' cDNA. Capped *Otp* mRNA was in vitro-transcribed with Sp6 RNA polymerase from the three recombinant plasmids linearized with *Not*I restriction enzyme.

### mRNA injection and embryo staining

In vitro-transcribed wild-type and deletion mutant mRNAs were extracted and ethanol-precipitated. mRNAs were resuspended in 10%



**Fig. 2.** Determination of gene number. Southern blot of DNA from three male individuals of sea urchin digested with the *EcoRI* restriction enzyme. The drawing indicates the structure of the cDNA and of the probe. HD, homeodomain.



indicating the presence of homozygotic and heterozygotic alleles, respectively.

The temporal expression profile of *PlOtp* was investigated by RNA blot analysis. As shown in Fig. 3, a single mRNA band appeared in embryos at relatively late stages of development. *Otp* transcripts were not detected in early cleavage stages. Following 2 weeks exposure of the gel blot, a faintly hybridizing RNA band was observed at the early gastrula (EG) stage (20 hours of development) (Fig. 3). These observations suggested that *Otp* is a zygotic gene which is activated by the onset of gastrulation. *Otp* transcripts abruptly increase in abundance at the prism (P) stage (30 hours of development), and are maximally expressed in the pluteus larva (PL; 53 hours of development). A low level of transcription of the *Otp* gene also occurs in adult tissues, including lantern and tubefeet, but no transcripts were detected in adult intestine or coelomocytes.

**Fig. 4.** Localization of *Otp* transcripts detected by whole-mount in situ hybridization. (A) Ventral view of a mid-gastrula embryo showing expression in two pairs of ventrolateral cells, symmetrically positioned with respect to the archenteron. (B-C) Mid-gastrula embryos viewed along the animal-vegetal axis. Stained cells are localized in the ventrolateral ectoderm, corresponding with the PMC clusters (indicated by the red arrows in B). (C) The stained cells reside in the flattened oral side. (D) Lateral-vegetal view of a gastrula showing stained cells in the oral epithelium. (E) A late-gastrula showing an increased number (six) of *Otp*-expressing cells. (F) Oral view of a prism-stage embryo showing expression in the future anal arms (yellow arrows), in the oral hood at the place where the oral arms will bud off (blue arrowheads) and corresponding with the coelomic sacs (black arrows). (G) Two optical views of an embryo focused to give emphasis to the stained cells. The black asterisk indicates unspecific staining. The red arrow points to the row of *Otp*-expressing cells close to the tip of the budding anal arm; no expression occurs in ectoderm cells located at the center of the arms. (H) An early pluteus-stage embryo. *Otp* transcripts are localized as in F except for the presence of two more stained cells flanking the foregut (white arrows). a, anus.

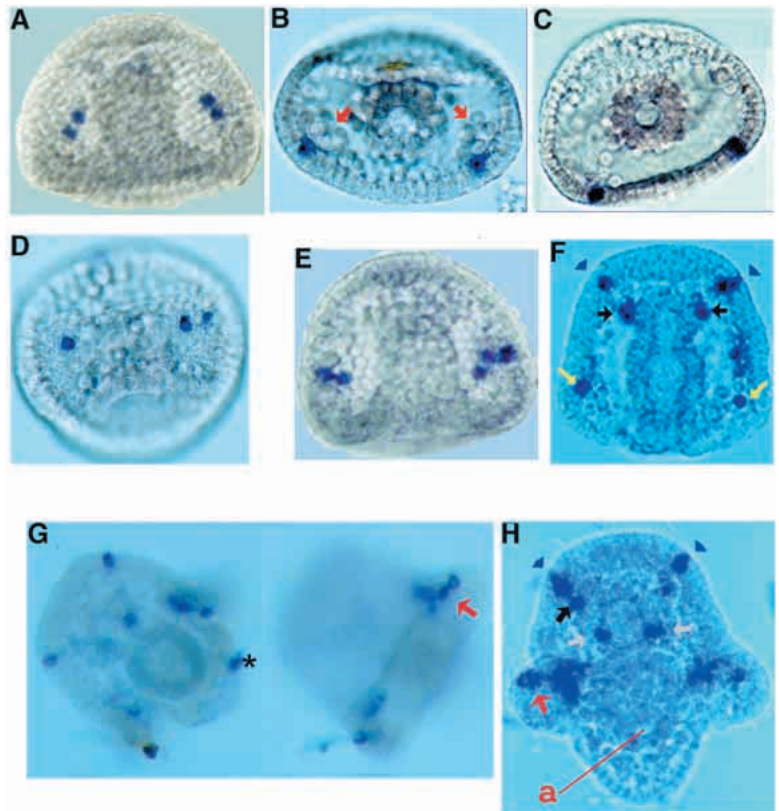
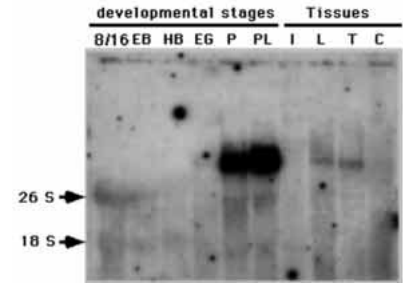


**Fig. 3.** *PlOtp* expression during embryogenesis and in adult tissues. Total RNA was from: 8- to 16-stage cell (8/16), early blastula (EB), hatching blastula (HB), early gastrula (EG), prism (P), plutei (PL), intestine (I), lantern (L), tubefeet (T) and coelomocytes (C). RNAs were fractionated by denaturing electrophoresis, blotted onto a nylon membrane and hybridized with an antisense-labelled *Otp* RNA. Arrows point to the 18S and 26S rRNA bands that unspecifically trapped some labelled probe. The blot has been exposed for 15 days to reveal the weak bands at the early gastrula stage and in the lantern and tubefeet adult organs.



**Localization of *Otp* transcripts during embryogenesis**

To determine the spatial expression pattern of *Otp* during embryogenesis, we performed whole-mount in situ hybridization using RNA probes labelled with digoxigenin (DIG). No stained cells were detected in control embryos hybridized to a sense probe (data not shown). With an antisense probe, *Otp* transcripts were detected at later stages of development as shown in Fig. 4. At the gastrula stage, most embryos exhibited a few labelled cells symmetrically positioned on both sides of the archenteron. *Otp*-expressing cells were localized to the oral epithelium. This is particularly evident when the embryos are viewed along the animal-vegetal axis (Fig. 4B,C) or from a lateral-vegetal view (Fig. 4D). *Otp*

transcripts are first detected in cells adjacent to ventrolateral PMC clusters (arrows, Fig. 4B), where skeleton production is initiated (Wilt, 1987). Results of in situ hybridization of embryos at prism and pluteus stages indicated that the number of labelled cells increases as development proceeds. In addition, they confirm the oral ectodermal lineage of cells expressing *Otp*. Cells expressing *Otp* always exhibited left/right symmetry with a mirror image pattern, and were not found in aboral ectoderm. High levels of *Otp* expression occur in ectoderm cells flanking the oral hood in the ventrolateral ectoderm at the animal pole (blue arrowheads, Fig. 4F,H). These stained cells are adjacent to the site where the oral (anterolateral) arms will bud off. *Otp*-expressing cells were also found close to the coelomic sacs (black arrows, Fig. 4F). At the early pluteus stage, the pattern of *Otp*-expressing cells remains similar. A row of three stained cells were found near each tip of the budding postoral (anal) arms (red arrows, Fig. 4G,H), and two cells were observed flanking the foregut (white arrows, Fig. 4H). There is a striking correspondence between sites of active skeletal rod growth in the ventral region and the distribution of *Otp*-expressing ectodermal cells.

### Expression of *Otp* in vegetalized and ventralized embryos

The expression pattern just described suggests that *Otp* might be involved in skeletal morphogenesis. To test this hypothesis, we performed in situ hybridization experiments on embryos vegetalized by lithium treatment. The teratogenic effects of this chemical on the sea urchin embryo have been well studied. In most cases, exogastrulated larvae are produced whose morphology is characterized by an increase in endoderm and mesoderm at the expense of ectoderm, and by a shift of primary mesenchyme cells toward the animal pole (reviewed in Gustafson and Wolpert, 1963). The phenotype of *P. lividus* embryos at 46 hours of development raised in the presence of 30 mM lithium ion is shown in Fig. 5A. A spherical ectodermal mass containing an aberrant spicule is clearly evident at the animal pole (Fig. 5A1). In lithium-treated embryos, *Otp*-expressing cells were shifted along the animal-vegetal axis in a manner analogous to that seen for PMCs. Most commonly, one or two symmetrical pairs of positive cells were observed (Fig. 5A2,A3 and results not shown). In addition, lithium treatment caused a reduction in the number of *Otp*-expressing cells. Rather than approximately 18 cells expressing the *Otp* gene in unperturbed prism embryos (Fig. 4), a maximum of four stained cells was detected in lithium-treated embryos. This observation correlates well with the reduction of ectoderm-derived structures and cleavage rate in embryos vegetalized by LiCl treatment (Hägstrom and Lönning, 1967). The finding that *Otp* transcripts are specifically confined to oral ectoderm prompted us to examine their distribution in ventralized sea urchin embryos. As previously demonstrated, chemical treatment of embryos with 0.5 mM NiCl<sub>2</sub> causes disruption of the O-A axis, resulting in an over-representation of oral ectoderm cells and a consequent increase in expression of EctoV, an oral ectoderm marker (Hardin et al., 1992; Armstrong et al., 1993). Fig. 5B shows the distribution of *Otp* RNA in embryos at 30 hours (Fig. 5B1,B2) and 39 hours (Fig. 5B3) of development. Two features are clearly evident. In contrast to unperturbed embryos, stained cells in nickel-treated embryos adopt a radialized pattern. In addition, in several

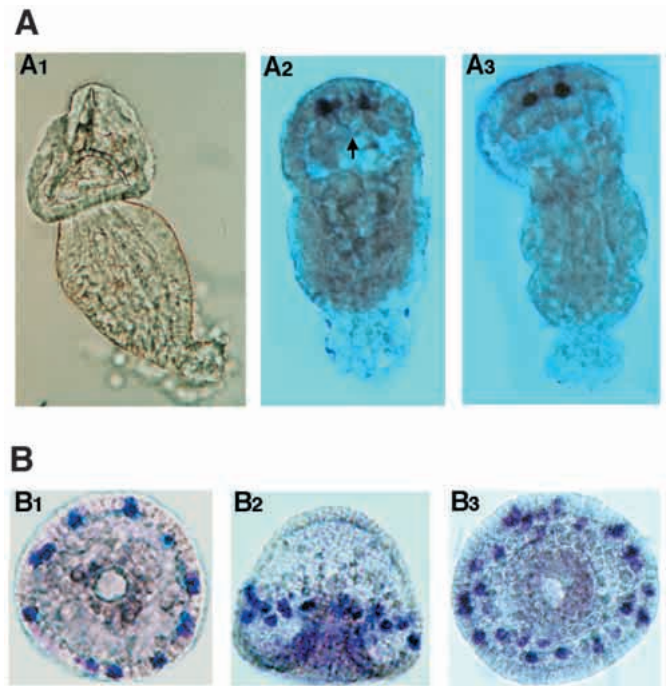


**Fig. 5.** Effects of lithium and nickel ions on the expression of the *Otp* gene. (A) Embryos were vegetalized by exposure to 30 mM LiCl from fertilization to the blastula stage. After that, embryos were cultured in MFSW till 46 hours of development. (A1) Brightfield image of an exogastrula. In the reduced ectoderm, at the animal pole, a large spicule is present. (A2,A3) Two embryos showing one pair of stained cells in the ectoderm overlying the PMC clusters (arrow in A2). (B) Sea urchin embryos, raised in the continuous presence of 0.5 mM NiCl<sub>2</sub> added after fertilization, were fixed and hybridized with the *Otp* antisense probe. (B1,B2) 30-hour post-fertilization embryos viewed along the A/V (Animal/vegetal) axis (B1) and from the oral side (B2). (B3) A 39-hour post-fertilization embryo showing an increased number of *Otp*-expressing cells.

embryos the number of *Otp* expressing cells is increased (Fig. 5B3), almost doubling in some cases (not shown) as compared to unperturbed embryos at the same developmental stage. In other embryos this increase is less pronounced. Variation in the number of *Otp*-expressing cells is likely to depend on a variable response to NiCl<sub>2</sub> in individual embryos.

### *Otp* misexpression and oral ectoderm patterning

Results described in foregoing sections suggested that *Otp* might be involved in the initiation of skeleton formation. If this is the case, ectopic expression of *Otp* would be expected to induce multiple spicule initiation sites in late cleavage embryos. We microinjected roughly 1 pl of *Otp* mRNA at 1 pg/nl into the cytoplasm of *P. lividus* or *S. granularis* unfertilized eggs. Consequent developmental defects were identical for both sea urchin species. Following fertilization, embryos were raised and collected at 44 hours or 72 hours for microscopic observation. Control sibling embryos injected with glycerol solution were normal plutei, exhibiting the characteristic bilateral skeletal pattern (not shown). A majority of *Otp*-injected embryos presented defects in spiculogenesis and exhibited a radialized skeleton (Fig. 6A). Similar morphological alterations were observed by injecting 0.5 pg of

mRNA. A fourfold increase in *Otp* mRNA, up to 4 pg/pl, resulted in an augmented number of embryos with arrested development (not shown). Control experiments demonstrated that the abnormal phenotypes were due to a specific effect of *Otp* misexpression. Microinjection of 4 pg of a truncated *Otp* mRNA encoding for the N terminus and the first eight amino acids of the homeodomain had no effect on development (Fig. 6B). Identical results were obtained by injecting the same amount of a deletion mutant encoding the C-terminal region of *Otp* (not shown). As shown in Fig. 7, the most striking effect seen in the majority of *Otp*-injected embryos at 44 hours of development was the radial distribution of skeleton rods (Fig. 7A,B,E) around the archenteron. Other embryos presented supernumerary triradiated spicules regularly spaced in the blastocoele (Fig. 7C,D). Remarkably, by 3 days of development, *Otp*-injected embryos showed abnormal skeleton rods that grew in an unpredictable pattern. In some embryos, they formed an irregular radial structure that branched in several directions (Fig. 7F,G-I).

The major morphological defects caused by *Otp* mRNA injection were the destruction of normal PMC patterning and the formation of a radial skeleton. As these effects recall those caused by nickel treatment, we hypothesized that *Otp* misexpression could also ventralize embryos, resulting in an increase in size of the oral territory. To address this issue, we examined the expression of the oral ectoderm specific marker EctoV (Coffman and McClay, 1990).

Control plutei were immunostained with the EctoV monoclonal antibody in the oral region (Fig. 7J'). In contrast to its distribution in control plutei, EctoV was radially expressed in *Otp* mRNA microinjected embryos (Fig. 7H',I'). These results strongly suggest that *Otp* specifies the positional identity of ectodermal cells along the O-A axis.

In different experiments, the proportion of *Otp* mRNA-injected embryos exhibiting aberrant skeletons ranged from 55% to 95%. To understand the reason for this variability, we examined the expression and distribution of *Otp* protein in microinjected embryos. Due to the lack of *Otp* antibody, we utilized a myc-tagged expression vector, CS2+MT (Turner and Weintraub, 1994), to make an in-frame fusion of the myc epitope to the coding region of *Otp*. As controls, the 5' and 3' deletion mutants of *Otp* were also cloned into CS2+MT. The mRNAs transcribed from these constructs were injected into embryos, and embryos at 44 hours of development were stained with anti-myc monoclonal antibody. Results are shown in

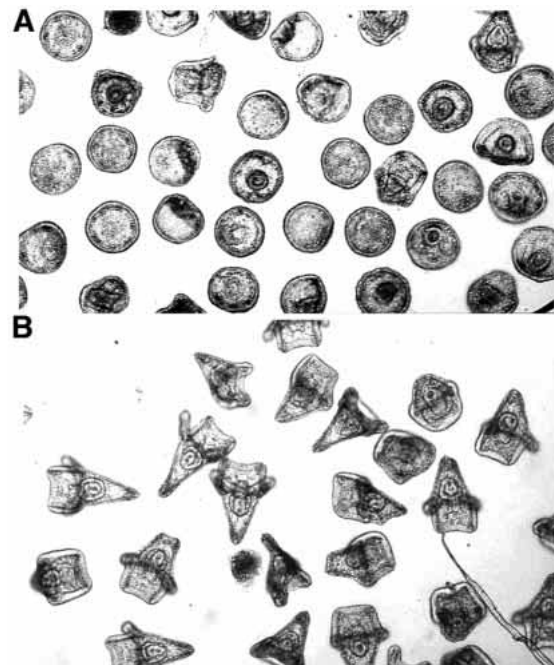


**Fig. 6.** Phenotypic effects of *Otp* mRNA injection. (A) View of embryos injected with 1 pg of *Otp* mRNA after 44 hours of development. (B) The same batch of embryos injected with 4 pg of the 3' deletion mutant, encoding for the N-terminal 123 amino acids.

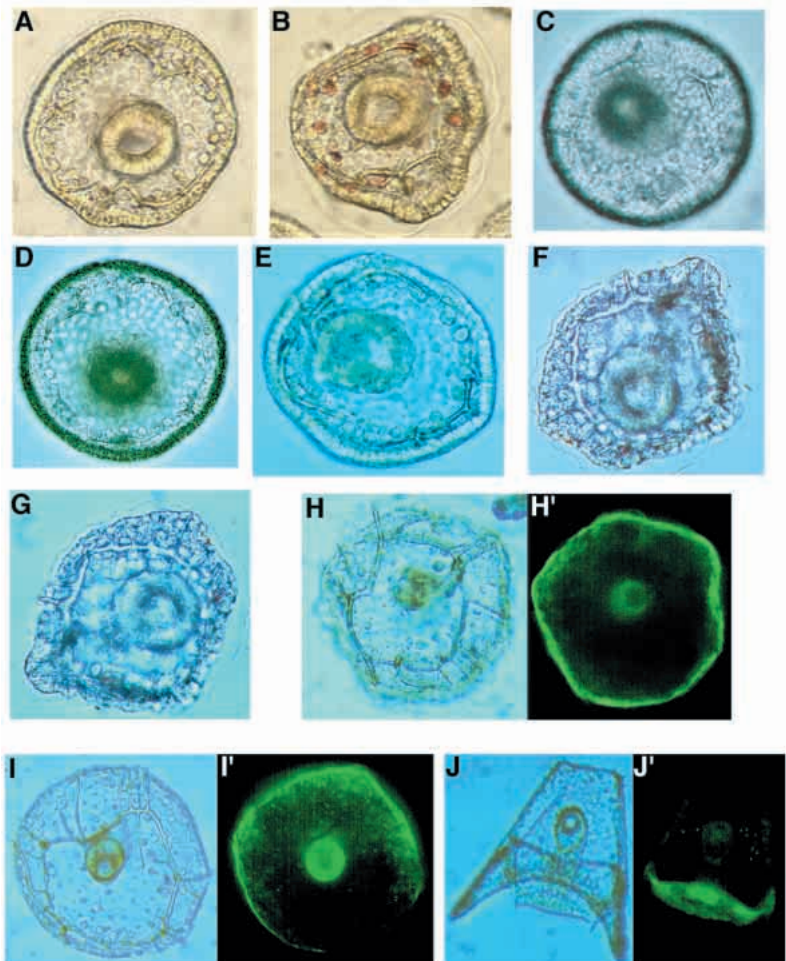


**Fig. 7.** *Otp* mRNA injection and alteration of skeleton patterning in *P. lividus* and *S. granularis* embryos. (A-G) *P. lividus* embryos viewed along the animal vegetal axis. The eggs were injected with 1 pg of *Otp* mRNA, fertilized and the embryos analyzed 44 hours (A-E) and 72 hours (F,G) after injection. (H,I) Brightfield images of two *S. granularis* embryos, after 72 hours of development, displaying a circular and highly branched skeleton pattern; (H', I') Fluorescence images of the embryos in H and I, showing the localization of the EctoV antigen. (J,J') Brightfield and EctoV fluorescence images, respectively, of a *S. granularis* normal pluteus.

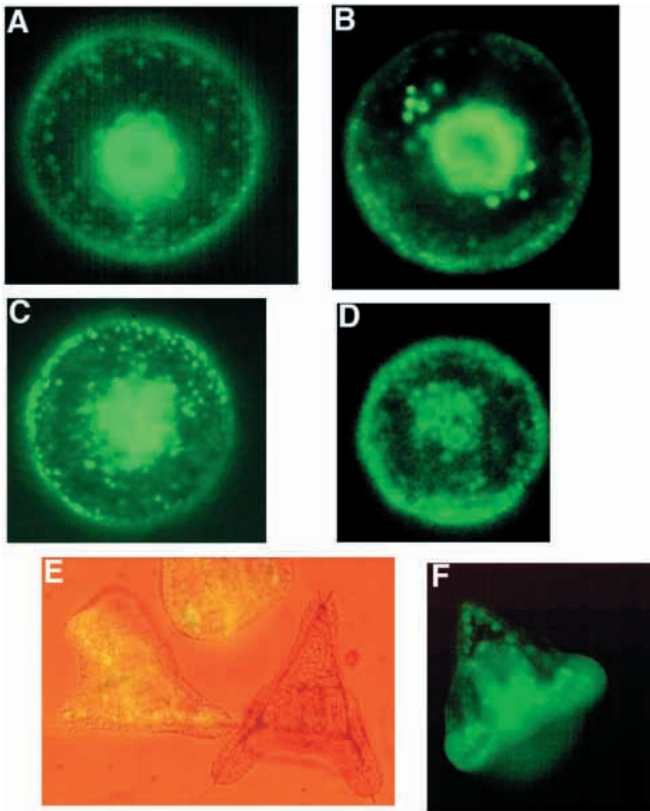


**Fig. 8.** Distribution of the myc-Otp fusion proteins in embryos microinjected with wild-type and mutant *Otp* mRNAs. (A-D) *P. lividus* embryos at 44 hours of development microinjected with 1 pg of wild-type *myc-Otp* mRNA and stained with an anti-c-myc antibody. The embryos exhibited supernumerary radial spicules (not shown). The protein was synthesized in all regions of the embryo, although the archenteron and some ectoderm cells were overstained, probably indicating a higher protein concentration. (E) Superimposed fluorescence and brightfield images of embryos at pluteus stage microinjected with the mutant RNA encoding for the N terminus. Two embryos show expression of *Otp*. Note the absence of background staining in the third embryo. (F) Embryo microinjected with the RNA encoding for the C terminus region. The *Otp* fusion protein is present in all regions of the embryo.

Fig. 8. Three effects were clearly evident. First, in radialized embryos, staining is almost uniformly distributed, although ectopic *Otp* protein was not present in every cell and was more abundant in some cell types (Fig. 8A-D). Second, embryos that presented a normal phenotype were unstained (not shown), indicating that either they escaped injection or that *Otp* mRNA, for unknown reasons, was not translated to appreciable levels. This variability in embryos positive for expression of ectopic protein was also observed in embryos injected with the mutant mRNAs, as shown in Fig. 8E. Finally, mutant *Otp* proteins were highly expressed in all regions of the embryos with no visible effects on development (Fig. 8E,F).

## DISCUSSION

### *Otp* is a stage- and tissue-specific zygotic gene

The sea urchin homologue of *Otp* was first isolated from *S.*

*purpuratus* by Simeone and coworkers utilizing a mouse probe (Simeone et al., 1994), but nothing was known about its expression or function during embryogenesis. In this paper we have described the isolation of the homologous gene from a *P. lividus* cDNA library and have presented data on its expression profile during embryogenesis. Sea urchin *Otp* is a single copy gene expressed at detectable levels from mid-gastrula onwards, producing a single transcript. This contrasts with the situation in the mouse where multiple RNA transcripts were detected and exhibited varying patterns during development (Simeone et al., 1994). *Otp* is also expressed at low levels in two adult tissues, lantern and tube feet.

### *Otp* expression and skeletogenesis

Transcription of the *Otp* gene begins around the time of extensive migration of PMCs that have entered the blastocoel. PMCs adopt a ring-like arrangement on the ectoderm near the vegetal pole. Some cells of the primary mesenchymal ring will cluster at the right and left corners of the ventral side to form the spicule rudiment. From there, triradial spicular arms arise and the skeleton of the larva will grow (reviewed in Gustafson and Wolpert, 1963; Okazaki, 1975). Expression of *PlOtp* displayed a remarkably restricted localization. In mid-gastrula stage embryos, transcription occurred in two ectodermal cell doublets, positioned in the ventrolateral regions of the embryo, proximal to the site where spicule primordium will initiate. The pattern of *Otp* expression at prism and pluteus stages of development reinforces the correlation between spiculogenesis and localization of *Otp* transcripts. The two halves of the skeleton and *Otp*-expressing cells in each half of the embryo are mirror images of one another. *Otp* transcripts were observed close to the tips of the anal and oral arms, where plugs of PMCs allow arm rod elongation (Gustafson and Wolpert, 1961b). Consistent with the correlation between skeleton rod growth and sites of *Otp* expression is the evidence that photoablation of ectodermal cells at arm tips caused inhibition of arm elongation (Ettensohn and Malinda, 1993).

Expression of *Otp* in early plutei was never found at the middle of the ventral side, where the ventral transverse (mid-ventral) rods arrest their growth (Guss and Ettensohn, 1997), or in aboral ectoderm cells adjacent to PMCs of the dorsal chain. Absence of *Otp* expression in the latter location might be interpreted as an indication of the different mechanisms of extension utilized by arm rods or by body and ventral transverse rods. While the former elongate by a plugging mechanism, body and ventral transverse rods elongate along patterned PMCs of the dorsal and ventral cellular chains respectively (reviewed in Gustafson and Wolpert, 1963).

*Otp* transcripts were also observed adjacent to the coelomic pouches and in the foregut. We do not understand the significance of this intriguing observation. However, the formation of the coelom is associated the fusion of the stomodeal ectoderm and the tip of the archenteron, which following perforation, will form the mouth (Gustafson and Wolpert, 1963). Therefore, it is tempting to speculate that *Otp* might be involved in this process.

### *Otp* may specify ectodermal patterning sites along the oral-aboral axis for skeletal morphogenesis

The idea that skeleton formation is determined by the ectoderm is more than 60 years old (von Ubisch, 1937). The

observation that in vegetalized embryos the symmetrical ectoderm thickenings and the primary mesenchyme cells are both shifted toward the animal pole (Gustafson and Wolpert, 1961a; Okazaki et al., 1962), further indicated that PMCs respond to pattern information expressed in the ectoderm. This is now a widely accepted view that is supported by several kind of experimental evidence. First, when donor migratory PMCs were transplanted into the blastocoel of younger embryos, they were patterned as those of the recipient embryo (Ettensohn and McClay, 1986). Second, in nickel-treated embryos the ventrolateral ectoderm thickenings expand and encircle the archenteron, and as a consequence PMCs also dispose radially around the archenteron and produce regularly placed supernumerary triradiated spicule elements (Hardin et al., 1992; Armstrong et al., 1993). Third, by microsurgical and cell transplantation experiments it was definitively shown that cell-cell signalling within the ectoderm is involved in the patterning of PMCs in the oral region (Armstrong and McClay, 1994; Guss and Ettensohn, 1997; Hardin and Armstrong, 1997).

Based upon our study, we suggest that the *Otp* homeodomain regulator is one of the local cues that specifies oral ectodermal patterning sites for spicule initiation. In fact, we observed that perturbation of axial positional information disrupts the distribution of oral ectodermal cells expressing *Otp*. In embryos vegetalized by LiCl, *Otp*-expressing cells were shifted along the animal-vegetal axis, as previously observed for PMCs. Remarkably, in response to NiCl<sub>2</sub> treatment, *Otp* was expressed in a radialized pattern of expression similar to that shown for the PMC marker gene *SM30*, which is highly transcribed at sites of active skeletal rod growth (George et al., 1991; Guss and Ettensohn, 1997). For both genes, nickel caused an increase in both levels of expression and in numbers of positively stained cells adopting a radialized pattern. As expression of *SM30* in transplanted PMC responds to local ectodermal cues (Guss and Ettensohn, 1997), these correlations strongly indicate that the *Otp* gene is involved in signalling from epidermal epithelium to primary mesenchyme cells. It has been suggested that the interaction of ectoderm derived signalling molecules with extracellular matrix (ECM) leads to the expression of *SM30* and hence to spiculogenesis (Ettensohn et al., 1997; Wilt, 1997). Interestingly, sea urchin embryos cultured in the presence of a monoclonal antibody against an ECM protein exhibit severe skeletal abnormalities (Zito et al., 1998). It remains to be seen whether *Otp* triggers the signal cascade that leads to transcriptional activation of the *SM30* gene.

The embryonic skeleton forms by branching and elongation from the two triradiate spicule rudiments in a predictable manner (reviewed in Ettensohn et al., 1997). The spatial pattern of the skeletal rods is dictated by the position of the PMCs in the blastocoel. Results presented in this paper have shown that regulation of skeletal patterning was severely affected following microinjection of *Otp* mRNA into developing embryos. In most injected embryos, spiculogenesis initiated at multiple points. Observed developmental defects were not a consequence of RNA toxicity, as injection of fourfold greater amounts of RNA encoding for *Otp* mutants lacking the homeobox region had no effects on development. As indicated by the almost uniform distribution of wild-type and mutant proteins,

abnormal spiculogenesis in injected embryos was due to ectopic *Otp* expression. From these results, we propose that ectoderm cells ectopically expressing *Otp* may transmit a signal to PMCs to initiate spiculogenesis.

The most common morphological alteration observed in a number of experiments was the formation of a ring-like skeleton structure. Two lines of evidence suggest that developmental defects exhibited by *Otp*-injected embryos were similar to those caused by nickel treatment. First, supernumerary spicule rudiments regularly spaced around the archenteron were observed in several embryos. Second, the embryos presented a preponderance of oral ectodermal tissues that assumed a radialized pattern. We could not test whether *Otp* over- or mis-expression altered aboral ectoderm territory in a reciprocal fashion, as aboral specific markers are not available for the two sea urchin species. We are currently attempting to clone aboral specific genes to examine this issue.

We believe that alterations in skeletal morphogenesis caused by ectopic expression of *Otp* were a consequence of respecifying oral ectodermal cells along the oral-aboral axis. Although more experiments are needed to firmly establish this point, the results described in this paper represent the first demonstration in the sea urchin of the possible involvement of a homeobox gene in cell specification along an embryonic axis. The O-A axis is set up by the two-cell stage (Cameron et al., 1989) but, as shown by the effects of nickel treatment, becomes committed by the onset of gastrulation (Hardin et al., 1992). In this regard, it is of particular significance that *Otp* expression occurs within the period of NiCl<sub>2</sub> sensitivity for disruption of the O-A axis (Hardin et al., 1992). In addition, nickel treatment perturbs the pattern of *Otp* expression, and ectopic expression of *Otp* and nickel treatment have similar effects on development.

Very recently, it has been shown that mis-expression of an *Msx*-related homeobox gene caused, among other developmental defects, a disruption in skeletal mesenchyme cell patterning (Tan et al., 1998). However, while ectopic expression of *Otp* produced radialized embryos, ectopic expression of *Msx* affected the arrangement of PMCs within the blastocoel and the shape of skeletal rods. These observations, and the fact that the temporal and spatial expression of the two homeobox genes are completely different, suggest that *Otp* and *Msx* may play distinct roles in skeletal morphogenesis. It would be interesting to see whether the spatial expression pattern of the two homeobox genes can be influenced in a reciprocal fashion.

In conclusion, taken together our results support the hypothesis that the *Otp* transcription factor regulates the expression of genes that signal short range patterning information from ectoderm cells to PMCs. Identification of *Otp* target genes should allow us to gain further insight into processes involved in oral ectodermal patterning.

We are grateful to Dr A. Simeone for the gift of an *Otp* cDNA subclone and to Prof. D. McClay for sending us the EctoV monoclonal antibody. Many thanks also to Dr G. Duro for providing the cDNA library and to Dr S. Evans for reading and editing the manuscript. This work was supported by grants of MURST (Ministero dell'Università e della Ricerca Scientifica e Tecnologica, 60% and Cofinanziamenti Programmi di Ricerca Scientifica di Interesse Nazionale, 97). The technical assistance of D. Cascino and G. Morici is acknowledged. *PIOpt* accession number, AJ007501.



## REFERENCES

- Angerer, L. M., Dolecky, G. J., Gagnon, M., Lum, R., Wang, G., Yang, Q., Humphreys, T. and Angerer, R. C. (1989). Progressively restricted expression of a homeobox gene within the aboral ectoderm of developing sea urchin embryo. *Genes Dev.* **3**, 370-383.
- Armstrong, N., Hardin, J. and McClay, D. R. (1993). Cell-cell interactions regulate skeleton formation in the sea urchin embryo. *Development* **119**, 883-840.
- Armstrong, N. and McClay, D. R. (1994). Skeletal pattern is specified autonomously by th primary mesenchyme cells in sea urchin embryo. *Dev. Biol.* **162**, 329-338.
- Bellomonte, D., Di Bernardo, M., Russo, R., Caronia, G. and Spinelli, G. (1998). Highly restricted expression at the ectoderm – endoderm boundary of PIHbox 9, a sea urchin homeobox gene related to the human HB9 gene. *Mech. Dev.* **74**, 185-188.
- Cameron, R. A., Fraser, S. E., Britten, R. J. and Davidson, E. H. (1989). The oral-aboral axis of a sea urchin embryo is specified by first cleavage. *Development* **106**, 641-647.
- Cameron R. A., Smith L. C., Britten R. J. and Davidson E. H. (1994). Ligand-dependent stimulation of introduced mammalian brain receptors alters spicule symmetry and other morphogenetic events in sea urchin embryos. *Mech. Dev.* **45**, 31-47.
- Chomczynski, P. and Sacchi, N. (1987). Single-step method of RNA isolation by guanidinium thiocyanate-phenol-chloroform extraction. *Anal. Biochem.* **162**, 156-159.
- Coffman, J. A. and McClay, D. R. (1990). A hyaline layer protein that becomes localised to the oral ectoderm and foregut of sea urchin embryos. *Dev. Biol.* **140**, 93-104.
- Cox, K. H., Angerer, L. M., Lee, J. J., Davidson, E. H. and Angerer, R. C. (1986). Cell lineage-specific programs of expression of multiple actin genes during sea urchin embryogenesis. *J. Mol. Biol.* **188**, 159-172.
- Di Bernardo, M., Russo, R., Oliveri, P., Melfi, R. and Spinelli, G. (1994). Expression of homeobox containing genes in the sea urchin (*Paracentrotus lividus*) embryo. *Genetica* **94**, 141-150.
- Di Bernardo, M., Russo, R., Oliveri, P., Melfi, R. and Spinelli, G. (1995). Homeobox-containing gene transiently expressed in a spatially restricted pattern in the early sea urchin embryo. *Proc. Natl. Acad. Sci. USA* **92**, 8180-8184.
- Dobias, L. S. Ma, L., Wu, H., Bell, J. R. and Maxon, R. (1997). The evolution of *Msx* gene function: expression and regulation of a sea urchin *Msx* class homeobox gene. *Mech. Dev.* **61**, 37-48.
- Dolecki, G. J., Wang, G. and Humphreys, T. (1988). Stage and tissue-specific expression of two homeobox genes in sea urchin embryos and adults. *Nucleic Acids Res.* **16**, 11543-11558.
- Emily-Fenouil, F., Ghiglione, C., Lhomond, G., Lepage, T. and Gache, C. (1998). GSK3beta/shaggy mediates patterning along the animal-vegetal axis of the sea urchin embryo. *Development* **125**, 2489-2498.
- Ettensohn, C. A., Guss, K. A., Hodor, P., G. and Malinda, K. M. (1997). The morphogenesis of the skeletal system of the sea urchin embryo. In *Reproductive Biology of Invertebrates*, Vol. VII (ed. J. R. Collier), pp. 225-265. Oxford and IBH Publishing Co. Pvt. Ltd. New Delhi, Calcutta.
- Ettensohn, C. A. and Malinda, K. M. (1993). Size regulation and morphogenesis: a cellular analysis of skeletogenesis in the sea urchin embryo. *Development* **119**, 155-167.
- Ettensohn, C. A. and McClay (1986). The regulation of primary mesenchyme cell migration in the sea urchin embryo: Transplantation of cells and latex beads. *Dev. Biol.* **117**, 380-391.
- Frohman, M. A., Dush, M. K. and Martin, G. R. (1988). Rapid production of full-length cDNAs from rare transcripts: amplification using a single gene-specific oligonucleotide primer. *Proc. Natl. Acad. Sci. USA* **85**, 8998-9002.
- Gan, L., Mao, C. A., Wikramanayake, A., Angerer, L. M., Angerer, R. C. and Klein, W. (1995). An orthodenticle-related protein from *Strongylocentrotus purpuratus*. *Dev. Biol.* **167**, 517-528.
- George, N. C., Killian, C. E. and Wilt, F. (1991). Characterization and expression of a gene encoding a 30.6-kDa *Strongylocentrotus purpuratus* spicule matrix protein. *Dev. Biol.* **147**, 334-342.
- Ghiglione C., G. Lhomond, T. Lepage and Gache, C. (1993). Cell-autonomous expression and position-dependent repression by Li<sup>+</sup> of two zygotic genes during sea urchin early development. *EMBO J.* **12**, 87-96.
- Giudice, G. (1973). *Developmental Biology of The Sea Urchin Embryo*, pp. 3-9, Academic Press, New York and London.
- Guss, K. A. and Ettensohn, C. A. (1997). Skeletal morphogenesis in the sea urchin embryo: regulation of primary mesenchyme gene expression and skeletal rod growth by ectoderm-derived cues. *Development* **124**, 1899-1908.
- Gustafson, T. and Wolpert, L. (1961a). Studies on the cellular basis of morphogenesis in the sea urchin embryo: Directed movements of primary mesenchyme cells in normal and vegetalized larvae. *Exp. Cell Res.* **24**, 64-79.
- Gustafson, T. and Wolpert, L. (1961b). Studies on the cellular basis of morphogenesis of the sea urchin embryo. Development of the skeletal pattern. *Exp. Cell Res.* **25**, 311-325.
- Gustafson, T. and Wolpert, L. (1963). The cellular basis of morphogenesis and sea urchin development. *Inter. Rev. Cytol.* **15**, 139-214.
- Hägstrom, B. E. and Lönning, S. (1967). Cytological and morphological studies of the action of lithium on the development of the sea urchin embryo. *Wilhelm Roux's Arch. Entw. Org.* **158**, 1-12.
- Hardin, J. and Armstrong, N. (1997). Short-range cell-cell signals control patterning in the oral region of the sea urchin embryo. *Dev. Biol.* **182**, 134-149.
- Hardin, J., Coffman, J. A., Black, S. D. and McClay, D. R. (1992). Commitment along the dorsoventral axis of the sea urchin embryo is altered in response to NiCl<sub>2</sub>. *Development* **116**, 671-685.
- Hörstadius, S. (1973) *Experimental Biology of the Echinoderms*. Oxford University Press.
- Manak, J. R. and Scott, M. P. (1994). A class act: conservation of homeodomain protein functions. *Development Supplement*, 61-71.
- Mao, C. A., Wikramanayake, A., Gan, L., Chuan, C., Summers, R. G. and Klein, W. H. (1996). Altering cell fates in sea urchin embryos by overexpressing SpOtx, an orthodenticle-related protein. *Development* **122**, 1489-1498.
- Martinez, P. and Davidson, E. (1997). *SpHmx*, a sea urchin homeobox gene expressed in embryonic pigment cells. *Dev. Biol.* **181**, 213-222.
- McGinnis, W. and Krumlauf, R. (1992). Homeobox genes and axial patterning. *Cell* **68**, 283-302.
- Okazaki, K. (1975). Normal development to metamorphosis. In *The Sea Urchin: Biochemistry and Morphogenesis* (ed. G. Cizihak), pp. 177-232. New York: Springer-Verlag.
- Okazaki, K., Fukushi, T. and Dan, K. (1962). Cyto-embryological studies of sea urchin IV. Correlation between the shape of the ectodermal cells and the arrangement of the primary mesenchyme cells in sea urchin larvae. *Acat Embryol. Morphol. Exp.* **5**, 17-31.
- Ramachandran, R. K., Wikramanayake, A. H., Uzman, J. A., Govindarajan, V. and Tomlinson, C. R. (1997). Disruption of gastrulation and oral-aboral ectoderm differentiation in the *Lytechinus pictus* embryo by a dominant/negative PDGF receptor. *Development* **124**, 2355-2364.
- Ransick, A. and Davidson, E. H. (1993). A complete second gut induced by transplanted micromeres in the sea urchin embryo. *Science* **259**, 1134-1138.
- Reynolds S. D., Angerer L. M., Palis J., Nasir A. and Angerer R. C. (1992). Early mRNAs, spatially restricted along the animal vegetal axis of sea urchin embryos, include one encoding a protein related to tolloid and BMP-1. *Development* **114**, 769-786.
- Simeone, A., D'Apice, M. R., Nigro, V., Casanova, J., Graziani, F., Acampora, D. and Avvantiato, V. (1994). *Orthopedia*, a novel homeobox-containing gene expressed in the developing CNS of both mouse and *Drosophila*. *Neuron* **13**, 83-101.
- Tan H., Ransick A., Wu H., Dobias S., Liu Y. H. and Maxson R. (1998). Disruption of primary mesenchyme cell patterning by misregulated ectodermal expression of SpMx in sea urchin embryos. *Dev. Biol.* **201**, 230-246.
- Tomlinson, C. R. and Klein, W. H. (1990). Temporal and spatial transcriptional regulation of the aboral ectoderm-specific *Spec* genes during sea urchin embryogenesis. *Mol. Reprod. Dev.* **25**, 328-338.
- Turner, D. L. and Weintraub, H. (1994). Expression of achaete-scute homolog 3 in *Xenopus* embryos converts ectodermal cells to a neural fate. *Genes Dev.* **8**, 1434-1447.
- von Ubisch, L. (1937). Di Normale Skelettbildung bei *Echinocyamus pusillus* und *Psamechinus miliaris* und die Bedeutung dieser Vorgänge für die Analyse der Skelette von Keimblatt-Chimären. *Z. Wiss. Zool.* **149**, 402-476.
- Wilt, F. H. (1997). Looking into the sea urchin embryo you can see local cell interactions regulate morphogenesis. *BioEssays* **19**, 665-668.
- Zito, F. Tesoro V., McClay D. R., Nakano, E. and Matranga, V. (1998). Ectoderm Cell-ECM Interaction is essential for sea urchin embryo skeletogenesis. *Dev. Biol.* **196**, 184-192.